

MONDAY, SEPTEMBER 3RD 2012

209. Pulmonary circulation and functional lung imaging

P1692

Simultaneous imaging of lung structure and function with triple nuclear MRI
 J.M. Wild¹, Helen Marshall², Graham Norquay³, Peggy Xu⁴,
 Juan Parra-Robles⁵. ¹Academic Radiology, University of Sheffield, United Kingdom

Rationale: In this work, we re-engineer a standard clinical MRI scanner to allow spatially registered human lung imaging from three different nuclei simultaneously with 1H anatomical images and hyperpolarized 3He and 129Xe lung ventilation images.

Methods: This is achieved by the use of geometrically nested, decoupled radio-frequency (RF) coil hardware resonating at the respective resonant frequencies. Multi-nuclear RF transmission and reception is achieved by rapid switching (<10 ms) between the signals from the respective nuclei. The technique is demonstrated with simultaneous imaging of 3He, 129Xe and 1H in the lungs of healthy normal's following an inhalation of a 1 litre bag of gas containing 300 ml 3He and 400 ml N2

Main results: See Fig. 1 Images of 1H, 3He (red), and 129Xe (blue) acquired from a healthy volunteer in the same breath containing 300 ml of 129Xe and 300 ml of 3He; the anatomical 1H images show excellent spatial registration with the 3He and 129Xe ventilation images as demonstrated by the overlaid fused image (purple).

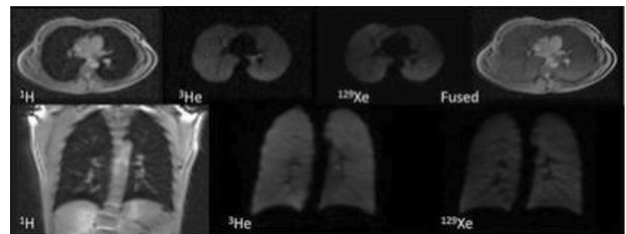


Figure 1

Conclusions: The precise temporal and spatial registration of these images is impossible to achieve in separate breath-hold scans. This new system opens up the possibility of simultaneous capture of regional lung function by exploiting the different properties of 3He and 129Xe gases (eg different diffusivities) with lung structure and anatomy from the 1H MRI without reliance on ionizing radiation.

P1693

PET imaging with [¹¹C]PBR28 and [¹⁸F]FDG distinguishes macrophage from neutrophil lung inflammation

Delphine Chen¹, Eugene Agapov², Kiran Solingapuram¹, Jacquelyn Engle¹, Elizabeth Griffin¹, Steven Brody², Jason Woods¹, Robert Mach¹, Richard Pierce², Michael Holtzman². ¹Mallinckrodt Institute of Radiology, Washington University School of Medicine, St. Louis, MO, United States; ²Internal Medicine/Division of Pulmonary and Critical Care Medicine, Washington University School of Medicine, St. Louis, MO, United States

Introduction: Noninvasive methods for quantifying macrophage and neutrophil activation and recruitment in chronic obstructive pulmonary disease (COPD) would be highly useful in assessing the efficacy of anti-inflammatory therapies.

Objective: To test whether positron emission tomography (PET) imaging with [¹¹C]PBR28 and [¹⁸F]fluorodeoxyglucose ([¹⁸F]FDG) could distinguish macrophage-dominant from neutrophilic inflammation in a mouse model of COPD. **Methods:** C57BL/6J mice inoculated with PBS or Sendai virus were imaged by microPET (Inveon or Focus 220, Siemens/CTI) with both [¹¹C]PBR28 and [¹⁸F]FDG at Days 3 and 84 post-inoculation (p.i.). Regions of interest placed over the lungs determined the % injected dose per cc (%ID/cc) at 60 min. Lung sections were stained for TSPO ([¹¹C]PBR28 ligand), Ly6G (neutrophil marker) and CD68 (macrophage marker).

Results: Only [¹⁸F]FDG uptake increased significantly during acute illness at p.i. Day 3. Both [¹¹C]PBR28 and [¹⁸F]FDG uptake increased significantly during chronic disease at p.i. Day 84. The [¹¹C]PBR28:[¹⁸F]FDG ratio, calculated for each mouse, was no different between infected (1.9±0.3) and uninfected mice (2.0±0.4) at p.i. Day 3. This ratio increased significantly at p.i. Day 84 (3.1±0.9) in infected mice compared to controls (1.7±0.5). Lung sections showed macrophages with intense TSPO staining at p.i. Day 84.

Conclusion: PET imaging with [¹¹C]PBR28 and [¹⁸F]FDG quantitatively distinguishes macrophage-dominant from neutrophilic inflammation in a mouse model of COPD. This approach may be useful for monitoring the pulmonary macrophage burden in humans with COPD, thereby guiding emerging targeted anti-inflammatory therapies.

P1694

³He MRI in young adults with congenital diaphragmatic hernia: Alveolar size differences between lungs

Marjolain Spoel¹, Helen Marshall², Hanneke IJsselstijn¹, Juan Parra-Robles², Piotr Wielopolski³, Els van der Wiel³, Andrew Swift², Smitha Rajaram², Dick Tibboel¹, Harm Tiddens³, Jim Wild². ¹Intensive Care and Pediatric Surgery, ErasmusMC/Sophia Childrens Hospital, Rotterdam, Netherlands; ²Academic Radiology, University of Sheffield, United Kingdom; ³Pediatrics-Respiratory Medicine and Allergology, ErasmusMC/Sophia Children's Hospital, Rotterdam, Netherlands

Rationale: To assess if compensatory lung growth occurs in neonatally operated congenital diaphragmatic hernia (CDH) patients with lung hypoplasia.

Objectives: To measure alveolar dimensions using hyperpolarised ³He MRI (Sheffield) in the hypoplastic and contralateral lung in Dutch adult CDH patients. **Methods and Measurements**

In 9 patients with left-sided CDH (born 1975-1993) lung function was measured. ³He MRI was used to image regional ventilation and to compute apparent diffusion coefficient (ADC) for ipsilateral (left) and contralateral lung separately.

Main results: Patients were ventilated neonatally for a median (range) of 7 (1-141) days. One patient needed extracorporeal membrane oxygenation (ECMO). Mean (SD) SDS FEV₁ -1.47 (0.96), SDS TLC_{pleth} -0.21 (1.16), RV%TLC_{pleth} 25.3 (4.48), SDS K_{COc} was -0.55 (0.79). ³He MRI showed ventilation abnormalities in 6 patients, ranging in severity from a single ventilation defect on ipsilateral side (n=3) to multiple ventilation defects in both lungs (ECMO treated patient, image). Elevated ³He ADC values in the ipsilateral lung were observed in 8 patients (Figure).

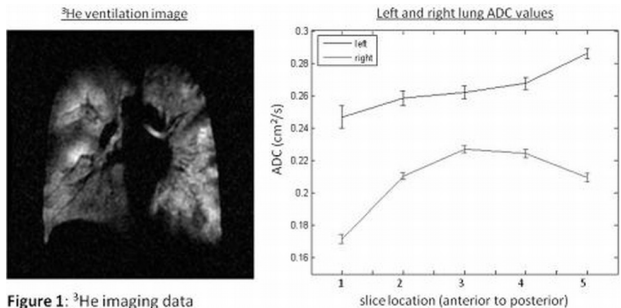


Figure 1: ³He imaging data

Conclusions: ³He MRI showed ventilation defects and substantial left/right ³He ADC differences, consistent with functional and micro-structural changes associated with lung hypoplasia in CDH. Contralateral ADC values in normal range suggest that compensatory lung growth occurred.

P1695

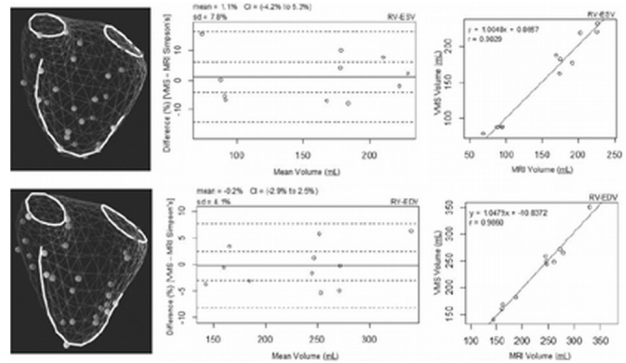
Three-dimensional reconstruction of the right ventricle from two-dimensional echocardiographic images: Validation of volume measurements against MRI

Nicole Bhawe¹, Benjamin Freed¹, Amit Patel¹, Megan Yamat¹, Lynn Weinert¹, James Bodtke², Roberto Lang¹, Mardi Gomberg-Maitland¹. ¹Medicine and Radiology, University of Chicago Medical Center, Chicago, IL, United States; ²R&D, VentriPoint Diagnostics, Seattle, WA, United States

Assessment of right ventricular (RV) function is an essential component of the diagnosis and management of patients with Pulmonary Arterial Hypertension (PAH). Today, this assessment is performed using two-dimensional echocardiography (2DE), which is challenging due to the complex geometry of the right ventricle. We hypothesized that 3D reconstruction of RV endocardium from 2DE images would provide accurate RV volume measurements. The aim of this study was to validate these measurements in against cardiac magnetic resonance (CMR) reference.

Methods: Eleven PAH patients were recruited for same day 2DE and CMR imaging. 2DE images of the right ventricle were acquired in standard imaging planes using a 3D spatial localization device. 3D reconstruction was performed using dedicated software to obtain end-systolic and end-diastolic volumes (ESV, EDV). (VentriPoint). CMR images were analyzed to provide RV volume reference values using Simpson's method of disks.

Results: Image acquisition was feasible in all 11 patients allowing reconstruction of the ventricular cast and volume measurements at end-systole and end-diastole.



Both ESV and EDV correlated highly between modalities. Bland Altman analysis showed minimal biases and narrow limits of agreement.

Conclusion: This study indicates that this novel technique may provide accurate measurement of RV volumes in PAH patients.

P1696

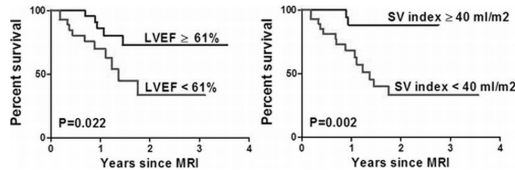
Prognostic value of ventricular volumes and function in patients with pulmonary hypertension due to chronic obstructive pulmonary disease

Andrew Swift¹, Smitha Rajaram¹, Dave Capener¹, Sproson Tom¹, Charlie Elliot², Robin Condliffe², David Kiely², Jim Wild¹. ¹Academic Unit of Radiology, University of Sheffield, United Kingdom; ²Sheffield Pulmonary Vascular Disease Unit, Sheffield Teaching Hospitals NHS Trust, Sheffield, United Kingdom

Background: This study investigated the relationship between ventricular structure and function and survival in patients with pulmonary hypertension due to COPD (PH-COPD).

Methods: 55 patients were evaluated with cardiac magnetic resonance imaging, right heart catheterization, lung function and CT emphysema scoring. Cardiac gated CINE MR and phase contrast imaging sequences were acquired in all patients. During follow-up of 42 months, 16 patients died. Cardiac volumes and function were analysed as predictors of mortality.

Results: Low SV measured by phase contrast MRI predicted mortality independent of demographic, haemodynamic, lung function and emphysema severity data (p=0.029). LVEF predicted mortality from univariate analysis (p=0.017), but did not reach significance at multivariate analysis (p=0.573). According to Kaplan-Meier survival curves, outcome was less favourable for patients with an inframedian SV index < 40 mL/m² (log rank; p=0.007), and worse outcome was associated with a LVEF <61%.



Right ventricular end-diastolic and systolic volume and left ventricular end-diastolic and end-systolic did not significantly predict mortality at Cox proportional hazards regression or Kaplan -Meier analysis.

Conclusions: Low SV is a strong predictor of adverse outcome in patients with PH-COPD. Static ventricular volumes did not aid the prediction of adverse outcome.

P1697

Quantitative estimation of lung perfusion scintigraphy in patients with chronic thromboembolic pulmonary hypertension and idiopathic pulmonary arterial hypertension

Olga Arkhipova, Tamila Martynyuk, Ludmila Samoilenko, Vladimir Sergienko, Irina Chazova. *Department of Systemic Hypertension, Russian Cardiology Research-and-Production Complex, Moscow, Russian Federation*

Aim: To estimate lung perfusion in patients with chronic thromboembolic pulmonary hypertension (CTEPH) and idiopathic pulmonary arterial hypertension (IPAH) by perfusion scintigraphy with technetium-99mm macroaggregated albumin.

Methods: The study included 54 pts with pulmonary arterial hypertension: 21pts (12 f/9m) with CTEPH and 33 pts with IPAH. Patients were comparable on age (45.7±12.5/37.5±10.5), WHO FC, systolic pulmonary artery pressure and distance in the 6 minute walking test. A 111-MBq dose of 99mTc-labeled macroaggregated albumin (99mTc-MAA) was injected into an cubital vein with the patient in a horizontal position. Just after, lung scanning was performed using a gamma-camera system Philips SKY LIGHT. Calculated including 99mTc-MAA in the upper, mean, lower zones of each lung and relation of the upper share to the lower was considered (U/L).

Results:

		CTEPH	IPAH
	Right lung, %	51.8±12.1	55.4±6.5
	Left Lung, %	47.6±12.0	44.1±6.7
Zone Vesta No. 1, %	Right lung	22.4±6.8	19.7±2.6
Zone Vesta No. 1, %	Left Lung	30.2±10.1 ¹	23.7±3.2
Zone Vesta No. 2, %	Right Lung	44.7±5.5	42.4±3.2
Zone Vesta No. 2, %	Left Lung	41.3±4.6	40.2±3.2
Zone Vesta No. 3, %	Right Lung	31.3±7.0	36.2±5.0
Zone Vesta No. 3, %	Left Lung	26.8±8.4 ²	34.7±5.0
U/L, %	Right Lung	0.74 (0.56-0.89)	0.52 (0.46-0.64) ³
U/L, %	Left Lung	1.02 (0.71-1.33)	0.69 (0.60-0.77)

¹p=0,004, ²p=0,0009, ³p<0,05.

Conclusions: Decrease of perfusion in the upper zone and decrease of U/L was revealed only in patients with IPAH. On the contrary CTEPH was characterized by increased in U/L. This finding may be helpful for differential diagnostics of pulmonary hypertension.

P1698

New insights into functional consequences of pulmonary embolism by cardiac MRI

Dirk Frechen¹, Stefan Krüger¹, Ingo Paetsch¹, Sebastian Kozerek², Bernhard Schnackenburg³, Michael Frick¹, Nikolaus Marx¹, Cosima Jahnke¹. ¹Internal Medicine I, University Hospital, Aachen, Germany; ²Institute for Biomedical Engineering, University of Zurich and Swiss Federal Institute of Technology, Zurich, Switzerland; ³Research Laboratories, Philips, Hamburg, Germany

Introduction: The objective of the present study was to evaluate a magnetic resonance imaging (MRI) algorithm which facilitates morphological diagnosis of pulmonary embolism (PE), right ventricular function and pulmonary perfusion (PP) in same examination.

Methods: 12 patients with documented PE on multidetector computed tomography (MDCT) and 14 healthy probands served as controls underwent multicomponent cardiovascular MRI. Diagnosis of PE was based on embolus visualization in MDCT. First, cine MRI was done employing multiple standard views. Second, high resolution, contrast-enhanced dynamic imaging of PP was performed. Third, a three-dimensional MRI angiography was acquired. Quantitative analysis of PP was derived from the signal intensity curve.

Results: In patients with PE compared to controls, RV ejection fraction was significantly lower (47.1±10.4% vs. 57.2±2.9%, p=0.002). Diagnosis of PE on a patient basis was 100% concordant between MDCT and MRI PP in MRI of areas affected by PE compared to normal lung areas showed a lower relative peak enhancement (172±157% vs. 542±213%, p<0.001), maximum peak enhancement (314±198% vs. 691±264%, p<0.001), wash-in rate (89±72a.u. vs. 184±77a.u., p<0.001), AUC (3212±2269 vs. 7215±3199, p<0.001) and a longer time-to-peak enhancement (17.5±6.9s vs. 9.5±3.0s, p<0.001).

Conclusions: Multicomponent cardiovascular MRI facilitated characterization of pulmonary arterial supply, RV function and PP during a single session examination and may serve as a profound basis for rapid clinical decision and for determination of therapeutic options in patients suspected of pulmonary embolism.

P1699

Cardiac magnetic resonance imaging versus echocardiography for assessment of cardiac involvement in pulmonary sarcoidosis

Teresa Fandl¹, Stefan Pfaffenberger¹, Karin Vonbank², Beatrice Marzluf², Julia Mascherbauer¹, Thomas Binder¹. ¹Dept. of Internal Medicine II, Division of Cardiology, Medical University of Vienna, Austria; ²Dept. of Internal Medicine II, Division of Pulmology, Medical University of Vienna, Austria

Study objectives: Data on the prevalence of cardiac involvement in sarcoidosis patients vary depending on the patient population and diagnostic modality studied. We aimed to compare cardiac involvement diagnosed by cardiac magnetic resonance imaging (CMR) with standard echocardiography and speckle tracking echocardiography for detection of cardiac sarcoidosis in patients with pulmonary sarcoidosis.

Methods: 41 patients (mean 47 years) with biopsy-proven pulmonary sarcoidosis underwent echocardiography and CMR imaging. Cardiac involvement was diagnosed if a positive late gadolinium enhancement (LE) pattern not typical for coronary artery disease on CMR was found. LE was compared to regional wall motion abnormalities on standard echocardiography and to global longitudinal peak systolic strain (GLPSS) on speckle tracking echocardiography. NT-proBNP was evaluated.

Results: No (0%) patient revealed cardiac involvement by echocardiography while 14 (34%) patients showed a positive LE on CMR (p<0.001). Four (10.5%) patients with positive LE showed a reduced GLPSS compared to 3 (7.9%) patients without LE (p=0.245). Mean NT-proBNP was higher in patients with positive LE (127 pg/ml), when compared to subjects without LE (87 pg/ml).

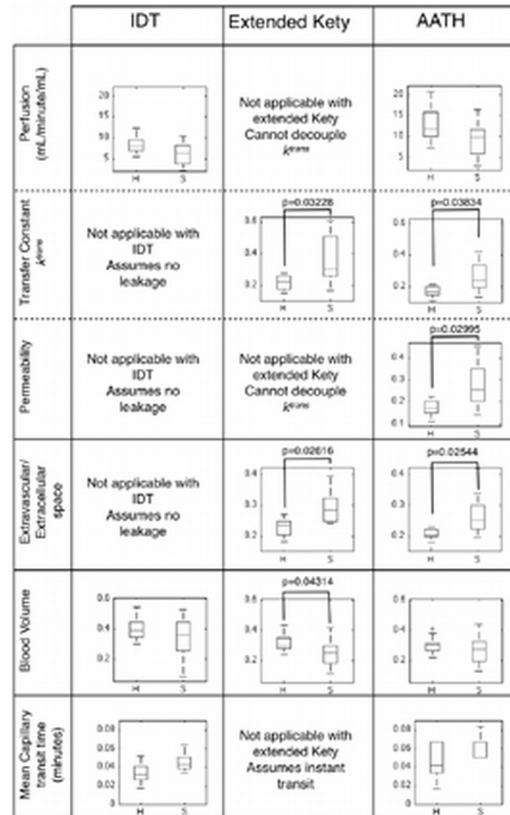
Conclusion: Cardiac involvement in pulmonary sarcoidosis patients was detected in more cases by CMR than by standard echocardiography. Speckle tracking echocardiography was also more sensitive than standard echocardiography. However, cardiac involvement in a caucasian population was rare compared to previously published data based on a predominantly afro-american population.

P1700

Comparison of dynamic contrast-enhanced MRI tracer-kinetic modeling in the lung of smokers v non-smokers

David Luke, Penny Hubbard, Geoff Parker, Josephine Naish. *Imaging Science and Biomedical Imaging, The University of Manchester, United Kingdom*

Previous analysis [1] of dynamic contrast-enhanced (DCE) MRI data in smokers v non-smokers using the extended Kety model revealed increased K^{trans} in smokers. By fitting the indicator dilution theory (IDT) and adiabatic approximation to the tissue homogeneity (AATH) models we hypothesise that we can decouple the contribution from perfusion and permeability to K^{trans} to yield enhanced information on lung function and changes due to smoking. Figure 1 summarises the results obtained from the three models used in the smoker study.



K^{trans} showed a significant difference between smokers and non-smokers from both the extended Kety ($p=0.032$) and AATH ($p=0.038$) models. The AATH model implies that the increase in K^{trans} is due to an increase in the permeability of the capillaries ($p=0.030$), rather than an increase in blood flow. Both the extended Kety ($p=0.026$) and AATH ($p=0.025$) models show a significant increase in the extracellular/extravascular space (EES) in smokers compared to non-smokers. In conclusion, the use of all three tracer-kinetic models indicate a coherent picture, supporting the hypothesis that increases in K^{trans} observed in smokers compared to non-smokers are related to increased capillary permeability rather than increased blood flow.

Reference:

[1] Naish JH et al, Proc. Intl. Soc. Mag. Reson. Med. 16 (2008) 401.

P1701

Simultaneous imaging of lung structure and function with triple nuclear MRI
 Jim Wild, Helen Marshall, Xiaoxun Xu, Graham Norquay, Juan Parra-Robles.
 Academic Radiology, University of Sheffield, United Kingdom

Hybrid medical imaging scanners (eg PET-CT) allow imaging with different detection modalities at the same time, providing complementary anatomical and functional information within the same physiological time course. Here, we re-engineer a standard clinical MRI scanner for the simultaneous acquisition of lung MR images from three different nuclei (1H, 3He and 129Xe) in a single breath-hold. The temporal and spatial registration of these images is impossible to achieve in separate breath-hold scans. This new system opens up the possibility of simultaneous capture of regional lung function from the 3He and 129Xe gases and lung structure from the 1H MRI without reliance on ionising radiation. Figure 1 shows images of 3He, 1H and 129Xe acquired from a healthy volunteer in the same breath; the anatomical 1H images show excellent spatial registration with the 3He and 129Xe ventilation images.

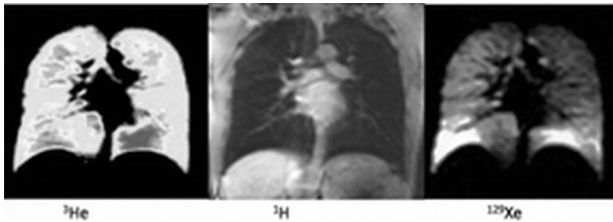


Figure 1

The method has multiple potential applications, allowing side-by-side quantitative analysis of early signs of impaired lung function from the 3He and 129Xe images and anatomical signs of disease from 1H MRI. For a variety of lung diseases, registration of ventilation MRI to anatomical 1H MRI would allow subsequent image registration to the radiological gold standard for anatomy, CT, which serves as the clinical gold standard in diseases such as emphysema.

P1702

Physiological modelling of dynamic contrast-enhanced MRI in COPD
 Penny Hubbard¹, Geoff Parker¹, Dave Singh², Jørgen Vestbo², Lars Olsson³, Lars Wigström³, Simon Young⁴, Eva Bondesson³, Josephine Naish¹. ¹Imaging Sciences Research Group/The Biomedical Imaging Institute, The University of Manchester, Manchester Academic Health Sciences Centre, Manchester, United Kingdom; ²Medicines Evaluation Unit, South Manchester University Hospital Trust, Manchester, United Kingdom; ³R&D, AstraZeneca, Mölndal, Sweden; ⁴R&D, AstraZeneca, Alderley Park, United Kingdom

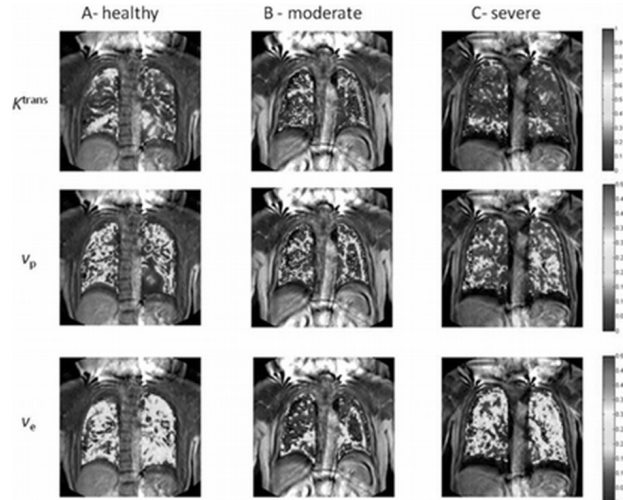
We present the results of a dynamic contrast-enhanced (DCE-) MRI study in subjects with COPD and age-matched healthy subjects. The pharmacokinetic model applied allows for extravasation of the contrast agent and can therefore be used to probe pulmonary capillary permeability.

Significant differences were not observed between healthy and moderate COPD groups in any of the DCE-MRI parameters. Significantly lower v_p and K^{trans} were observed in severe COPD compared with healthy and in v_p compared with moderate COPD (Fig. 1). v_e (extra-vascular/extra-cellular space) can be related to inflammation and shows a non-significant increase in moderate COPD.

Group mean and standard deviation of physiological DCE-MRI parameters

	Healthy	Moderate	Severe
K^{trans} (ml/ml tissue)/min	0.31±0.16	0.29±0.13	0.21±0.05 [†]
v_p , ml/ml tissue	0.22±0.11	0.22±0.09	0.14±0.04 ^{†‡}
v_e , ml/ml tissue	0.27±0.07	0.32±0.09	0.25±0.05

K^{trans} is related to perfusion and/or capillary permeability and decreases significantly in severe COPD. v_p (vascular space) also decreases with disease severity and, when considered in combination with decreased K^{trans} , is suggestive of reduced perfusion in the region analysed. This sensitivity to disease severity shows DCE-MRI may provide a novel window on the progression of COPD.



Abstract P1702 – Figure 1

P1703

Regional measures of 3D lung mechanics using magnetic resonance imaging
 Alexandra R. Morgan^{1,2}, Geoff J.M. Parker^{1,2,3}, Tim F. Cootes^{1,2}, Marietta L.J. Scott⁴, Josephine H. Naish^{1,2}. ¹Imaging Science, School of Cancer and Enabling Sciences, Manchester Academic Health Science Centre, University of Manchester, Greater Manchester, United Kingdom; ²Biomedical Imaging Institute, The University of Manchester, Greater Manchester, United Kingdom; ³BiOxyDyn, BiOxyDyn Limited, Manchester, United Kingdom; ⁴AstraZeneca R&D, Alderley Park, Macclesfield, United Kingdom

Lung disease, such as emphysema and fibrosis, can result in changes in pulmonary mechanical properties that are not easily identified on a regional level using current methods. A recently reported method, using 2D structural proton MRI in conjunction with post-processing and image registration, to provide measures of local lung motion and relative regional tissue compliance demonstrated differences between healthy and diseased lungs¹. This technique has been extended to 3D, to overcome the limitations of the 2D method.

Multi-slice structural lung MR images were acquired in 2 healthy volunteers during breath-hold at end-expiration and end-inspiration. 3D lung volumes were segmented, and an automatic mesh-based image registration used to identify correspondence points in the lung between the two respiratory extremes. Vector field maps of local lung motion show an increasing magnitude of motion from apex to diaphragm, as expected in healthy lungs, with motion in the anterior-posterior as well as in the foot-head direction (Figure 1). These methods provide potentially useful information on local lung mechanics in diagnosis of disease, and may be used to calculate regional lung compliance.

Reference:

[1] Morgan A.R. et al. ERJ 38:S55: p323s.

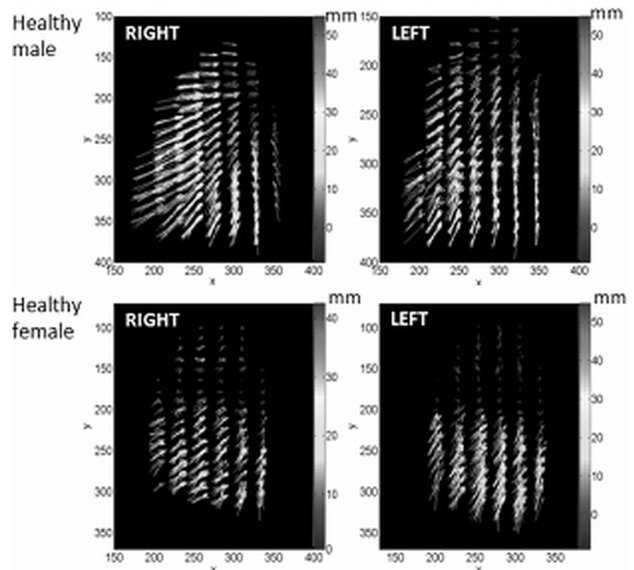


Figure 1. Vector field maps showing regional lung motion in expiration in a sagittal view. 3D motion is illustrated as vectors collapsed onto xy-plane. Vector length indicates magnitude of motion. x = anterior-posterior, y = foot-head.

MONDAY, SEPTEMBER 3RD 2012

P1704**Modelling of hyperpolarized gas diffusion in lungs of COPD patients and healthy volunteers using a fractional dynamics approach**

Juan Parra-Robles, Helen Marshall, Jim M. Wild. *Academic Radiology, University of Sheffield, United Kingdom*

MR diffusion experiments using hyperpolarized gas are sensitive to emphysema. However, interpretation of non-Gaussian diffusion is complicated by its dependence on a variety of factors (e.g. branching structure, susceptibility gradients, diffusion time, lung inflation and gas mixture composition) [Parra-Robles et al, JMR 204, 2010]. In this work, a theoretical model based in the application of fractional order dynamics to anomalous diffusion is presented. The model does not require assumptions about the geometry and distribution of apparent diffusion rates [Magin et al, JMR 190, 2008]. This technique can be used to quantify non-gaussian diffusion signals arising from a multiplicity of sources.

MR diffusion scans of eight healthy volunteers and 10 COPD patients were performed using hyperpolarised ³He. While the diffusivity (DDC) depended strongly on experimental conditions, the heterogeneity index α remained constant ($0.87 \pm 5\%$, in healthy volunteers), regardless of the diffusion time (in the range 1.6-2.5 ms), lung inflation, gas mixture and subject's size. Both, DDC and α were significantly different for the COPD patients. These results seem to indicate that α is insensitive to a range of uncertainties in experimental conditions but sensitive to changes in lung structure due to COPD.

Since the model is not constrained to a specific range of timing parameters, it may be able to reveal information about lung geometry from diffusion data acquired over different time scales. This information may be sensitive to lung diseases that affect airway morphology at different generations of the lung branching structure.

P1705**Distribution of airway closure using single photon emission computerised tomography in the obese**

Sriram Mahadev, Cheryl Salome, Gregory King. *Airway Physiology and Imaging, The Woolcock Institute of Medical Research, Glebe, NSW, Australia*

Low functional residual volume (FRC) in obesity may increase airway closure above FRC. Scintigraphic studies in obese patients with low expiratory reserve volume, showed reduced basal ventilation potentially due to airway closure (AC). We used single photon emission computerised tomography (SPECT-CT) to identify regional distribution of AC then related this to physiological measures of AC.

Hypothesis: (1) degree of AC occurring above FRC would correlate with area of closure seen on SPECT-CT, (2) the obese would have more AC particularly basally.

Methods: Obese subjects (OS n=5) and non-obese subjects (NOS n=7) had lung volumes (plethysmography), and single breath nitrogen washout to measure closing capacity (CC). CC/FRC > 1 indicated AC above FRC. SPECT-CT: 400mL of Technegas administered at FRC, inspiration to TLC. Areas of reduced Technegas deposition were defined as AC, and overall volume of AC, and volume of AC seen in upper, middle and bottom third of lung, expressed as a proportion of corresponding lung volume on CT (closure%).

Results: OS and NOS were well matched for age. OS had higher CC/FRC than NOS (not statistically significant: OS $93.6 \pm 18.5\%$, NOS $69.07 \pm 26.8\%$ p=0.11). There was no correlation between CC/FRC and overall closure% (r=0.22 p=0.5). OS did not have greater overall closure% than NOS. (NOS $19.5 \pm 4.2\%$, OS $19.52 \pm 11.3\%$ p=1). NOS had greater closure% in the upper third. (NOS $36.77 \pm 8.3\%$, OS $17.62 \pm 13.1\%$ p=0.03).

Conclusion: Surprisingly there were no differences in basal AC on imaging in the obese despite occurrence of AC above FRC. The reason is not known. Apparent AC in NOS compared to OS in upper zones may represent altered ventilation in the OS.

P1706**Synchrotron imaging of regional ventilation/perfusion- ratio after methacholine provocation in rabbit**

Liisa Porra¹, Mathieu Guilbart², Satu Strengell¹, Pekka Suortti¹, Anssi Sovijärvi³, Sam Bayat². ¹Department of Physics, University of Helsinki, Finland; ²Péritox-INNERIS and Pediatric Lung Function Laboratory, Université de Picardie Jules Verne, Amiens, France; ³Department of Clinical Physiology and Nuclear Medicine, Helsinki University Central Hospital, Helsinki, Finland

Rationale: K-edge subtraction (KES) CT imaging with synchrotron radiation allows quantitative measurements of regional ventilation (V) during xenon inhalation and regional blood volume (VB) distributions during iodine infusion. In this study, we assessed the feasibility of quasi-simultaneous KES imaging of V and VB.

Methods: Experiments were performed in anaesthetized and ventilated New Zealand rabbits (n=5). Images of V and VB were obtained at baseline and after inhaled MCh (125 mg/ml). Heterogeneity of both parameters was estimated as the coefficient of variation (CV) between pixels.

Results: Images of V, VB and their ratio (V/VB) are shown in one rabbit at baseline and after MCh challenge (Figure). Mch inhalation produced clustered areas of poor ventilation; mean V decreased to $75.7 \pm 24.2\%$ and VB to $69.4 \pm 12.7\%$ of baseline. The CV of V increased to $334 \pm 186\%$, CV of VB to $140 \pm 21\%$, and CV of V/VB ratio to $180 \pm 50\%$ of baseline. Values are m \pm SD, *significant change vs. baseline (P<0.05, Students paired t-test).

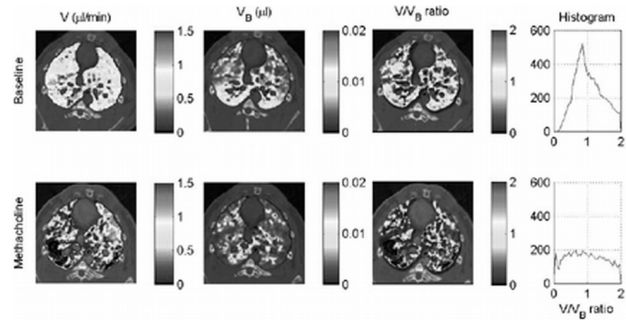


Figure 1

Conclusions: KES imaging allowed quasi-simultaneous measurement of regional ventilation and blood volume. Mch challenge caused significant changes in V and VB and increased the mismatch between the parameters. This method allows quantitative assessment of changes in regional V/VB ratio induced by drugs in models of asthma.

P1707**Scintigraphic parameters in bronchial asthma patients**

Tatyana Ageeva¹, Nikolay Krivonogov², Anna Dubodelova¹. ¹Propaedeutics of Internal Diseases Department, Siberian State Medical University, Tomsk, Russian Federation; ²Radiionuclide Diagnostics Laboratory, Cardiology Research Institute of Siberian Department of Russian Academy of Medical Sciences, Tomsk, Russian Federation

Aim: To study the ventilation-perfusion ratio (V/Q), apex-base gradient of ventilation (U/L-V) and perfusion (U/LQ) and alveolar-capillary permeability (ACP) in bronchial asthma (BA) patients on the basis of scintigraphy data.

Materials and methods: 30 people aged 18-60 took part in the study: patients diagnosed with BA (20) and healthy non-smoking volunteers (20). The scintigraphic studies were performed by means of Omega 500 gamma camera (Technicare, USA-Germany). The subject of the research was an examination of ACP in the right (RL) and left (LL) lungs in the process of radiopharmaceutical derivation, static conditions, during the 1st, 10th and 30th min after ^{99m}Tc DTPA inhalation.

Results: BA patients: V/Q in both RL and LL was not higher than 1.0 and amounted to 0.98 (0.92-1.04) in the RL and 0.98 (0.95-1.01) in the LL. These parameters did not differ from those of healthy volunteers (p=0.72 and p=0.65). U/L-V amounted to 0.55 (0.33-0.77) in the RL and 0.57 (0.45-0.69) in the LL. It was lower than that of healthy people (p=0.03 and 0.04). U/LQ amounted to 0.82 (0.66-0.98) in the RL and 1.1 (0.84-1.36) in the LL. This parameter was higher than that of healthy people (p=0.004, p=0.02). ACP in the RL amounted to 10.19% (6.49-14.19%) and 27.21% (22.99-31.41%) during the 10th and 30th minutes of the study, respectively; it was increased during the 30th minute (p=0.001). ACP in the LL amounted to 9.68% (8.49-10.87%) and 27.87 (24.26-31.48%) during the 10th and 30th minutes of the study, respectively; it was increased during the 30th minute of the study (p=0.002).

Conclusions: The study findings may serve as additional scintigraphic criteria for bronchial asthma diagnostics.

P1708**Quantitative CT-estimation of total and regional lung inflation in patients with bronchial asthma (BA)**

Andrey V. Il'in¹, Juliy M. Perelman¹, Anatoliy V. Lensis². ¹Laboratory of Functional Research of Respiratory System, Far Eastern Scientific Center of Physiology and Pathology of Respiration SB RAMS, Blagoveschensk, Russian Federation; ²Laboratory of Roentgen-Functional Research of Respiratory System, Far Eastern Scientific Center of Physiology and Pathology of Respiration SB RAMS, Blagoveschensk, Russian Federation

Background: Functional abnormalities are often the first and the only symptoms in BA. Spirometry do not allow lung inflation.

Aim: To estimate the potential of CT in identification of total and regional lung hyperinflation in BA patients.

Methods: 70 BA patients were examined compared with 20 healthy persons. The method of two stage multispiral CT by Activion 16 (Toshiba) with the further 3D-reconstruction and volumetry (-850 HU and lower) was used. The quantitative densitometric estimation at axial scanning in fixed upper, middle and lower lung zones was also done. Bronchodilation test with salbutamol inhalation was used.

Results: The lung dysfunction was registered in 66 patients. By 3D-volumetry, lung inflation at maximal expiration against inspiration in mild BA was $3.8 \pm 2.46\%$ (in healthy people - $0.3 \pm 0.55\%$, p<0.001), in moderate BA - $16.2 \pm 5.27\%$ (p<0.05 to mild BA) and in severe BA - $30.0 \pm 7.46\%$ (p<0.05 to moderate BA). By densitometry the mean expiration to inspiration ratio of density in mild BA was $80.0 \pm 3.14\%$ (in healthy people - $76.7 \pm 5.37\%$, p<0.01), in moderate BA - $85.0 \pm 3.48\%$ (p<0.05 to mild BA), in severe BA - $91.5 \pm 4.19\%$ (p<0.05 to moderate BA). After salbutamol inhalation patients with mild BA had a decrease of "air traps" volume: before the test the expiration to inspiration ratio of lung

MONDAY, SEPTEMBER 3RD 2012

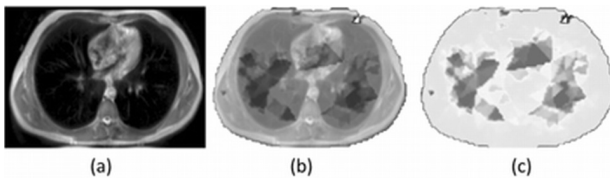
inflation was 7.3%, after the test - 2.3%; the quantity of voxels before the test was 3772 at inspiration, 276 at expiration, after the test - 4772 and 110, respectively).

Conclusion: By 3D-volumetry and densimetric analysis the conclusions about the lung inflation abnormality and the volume of "air traps" in BA patients can be drawn, which considerably supplements the spirometry.

P1709**MRI-informed electrical impedance tomography from phantom to thorax**

Ross Little¹, John Davidson², Josephine Naish¹, Paul Wright², Alexandra Morgan¹, Ron Kikinis³, Hugh McCann², Geoff Parker¹. ¹Imaging Science, University of Manchester, United Kingdom; ²School of Electrical and Electronic Engineering, University of Manchester, United Kingdom; ³Surgical Planning Laboratory, Brigham and Women's Hospital, Boston, MA, United States

Electrical impedance tomography (EIT) has the potential to provide non-invasive, high temporal resolution, long term lung function monitoring. We present an instrument capable of volumetric data acquisition applied to a male torso, show an MRI-informed reconstruction, and correspondence of EIT measurements with high resolution MRI.



EIT data were acquired using two planes of 16 electrodes on the Manchester fEITER system, a BS EN 60601-1:2006 compliant system, followed by MRI acquired using fast field echo on a 1.5 T Philips Achieva. The data were coaligned using the open source medical image platform 3D-Slicer. Figure 1(a)-(c) shows an MRI axial slice of the torso, coalignment with EIT, and EIT alone.

The system acquired volume data using 32 electrodes in two planes. The EIT was reconstructed using a torso boundary-only model derived from the MRI. This should produce a more faithful reconstruction than a generic model, allowing investigation of sensitivity of EIT measurements using increasingly precise models. At 100 fps, the EIT provides excellent temporal resolution. For example, it shows different temporal sequences of lung ventilation (dorsal versus ventral) within the breathing cycle for an upright subject as compared with supine. Current analyses of EIT data for lung function monitoring use sub-cycle statistics and time differentials; the (minimum) 3-fold increase in frame rate provided by fEITER will improve these methods substantially.